

Magnetic cycles of Sun-like stars with different levels of coronal and chromospheric activity — comparison with the Sun

Elena Shimanovskaya, Vasiliy Bruevich and Elena Bruevich

Sternberg Astronomical Institute, Moscow State University, Universitetsky pr., 13, Moscow 119992, Russia;
red-field@yandex.ru, brouev@sai.msu.ru, eshim@sai.msu.ru

Received 2015 November 26; accepted 2016 May 24

Abstract The atmospheric activity of the Sun and Sun-like stars is analyzed involving observations from the HK-project at the Mount Wilson Observatory, the California and Carnegie Planet Search Program at the Keck and Lick Observatories and the Magellan Planet Search Program at the Las Campanas Observatory. We show that for stars of F, G and K spectral classes, the cyclic activity, similar to the 11-yr solar cycle, is different: it becomes more prominent in K-stars. Comparative study of Sun-like stars with different levels of chromospheric and coronal activity confirms that the Sun belongs to stars with a low level of chromospheric activity and stands apart among these stars by its minimum level of coronal radiation and minimum level of variations in photospheric flux.

Key words: Sun: activity — Sun-like stars: activity

1 INTRODUCTION

Study of the magnetic activity of the Sun and Sun-like stars is of fundamental importance for astrophysics. This activity in stars leads to a complex combination of electromagnetic and hydrodynamic processes in their atmospheres. Local active regions, which are characterized by a higher value of intensity of the local magnetic field, are plagues and spots in photospheres, CaII flocculae in chromospheres and prominences in coronas.

Stars displaying irregular variations in their chromospheric emission possess more powerful coronas, while stars with cyclic activity are characterized by comparatively modest X-ray luminosities and ratios of the X-ray to bolometric luminosity L_X/L_{Bol} . This indicates that the nature of processes associated with magnetic-field amplification in the convective envelope changes appreciably in the transition from small to large dynamo numbers, directly affecting the character of the $(\alpha - \Omega)$ dynamo. Due to the strong dependence of both the dynamo number and the Rossby number on the speed of axial rotation, earlier correlations were found between various activity parameters and the Rossby number in Bruevich et al. (2001).

It is difficult to predict the evolution of each active region in detail. However, it has long been established that the total change in active areas integrated over the entire solar or stellar disk is cyclical not only in solar activity but also in stellar activity (see Baliunas et al. 1995; Kolláth & Oláh 2009; Morgenthaler et al. 2011; Bruevich & Kononovich 2011).

It is well known that the duration of the 11-yr cycle of solar activity (Schwabe cycle) ranges from 7 to 17 yr according to a century and a half of direct solar observations.

The most sensitive indicator of chromospheric activity (CA) is the Mount Wilson S -index (S_{HK}) - the ratio of the core of the CaII H&K lines to the nearby continuum (Vaughan & Preston 1980). Now the CaII H&K emission is established as the main indicator of CA in lower main sequence stars.

The HK-project at the Mount Wilson Observatory is one of the first and still one of the most outstanding programs acquiring observations that target Sun-like stars (see Baliunas et al. 1995; Lockwood et al. 2007). One of the most important results of the HK-project was the discovery of “11-yr” cycles of activity in Sun-like stars. Durations of CA cycles, found for 50 different stars of late spectral classes (F, G and K), vary from 7 to 20 yr according to HK-project observations.

Currently, there are several databases that include thousands of stars with measured fluxes in the chromospheric lines of CaII H&K emission cores (see Wright et al. 2004; Isaacson & Fischer 2010; Arriagada 2011; García et al. 2010, 2014). However, only for a few tens of stars are the periods of magnetic activity cycles known (Baliunas et al. 1995; Lockwood et al. 2007; Oláh et al. 2009; Morgenthaler et al. 2011).

In our work, we consider the following databases of observations of Sun-like stars with known values of S_{HK} :

- (1) The HK-project – the program in which the Mount Wilson S value was first defined. Later the Mount

Wilson “ S value” (S_{HK}) became the standard metric of CA – the basic value with which all future projects of stellar CA observations are compared and calibrated.

- (2) The California and Carnegie Planet Search Program which includes observations of approximately 1000 stars at Keck and Lick observatories in chromospheric CaII H&K emission cores. S_{HK} indexes of these stars are converted to the Mount Wilson system (Wright et al. 2004). From these measurements, median activity levels, stellar ages and rotation periods from general parameterizations have been calculated for 1228 stars, ~ 1000 of which have no previously published S -values.
- (3) The Magellan Planet Search Program which includes CA measurements of 670 F, G, K and M main sequence stars in the Southern Hemisphere taken at Las Campanas Observatory. S_{HK} -indexes of these stars are also converted to the Mount Wilson system (Arriagada 2011).

We believe that the stars in these databases are the best described stars which are similar to the Sun in terms of mass and evolutionary state. They are main sequence stars with a $(B - V)$ color between 0.48 and 1.00 (the Sun has a $(B - V)$ color of 0.66). Alternatively, a definition based on spectral type can be used, such as F5V through K5V.

The aims of our paper are: (1) a study of the location of the Sun among stars with different levels of chromospheric and coronal activity on the main sequence in the Hertzsprung-Russell diagram; (2) a comparative analysis of chromospheric, coronal and cyclic activity of the Sun and Sun-like stars with F, G and K spectral classes.

2 THE LOCATION OF THE SUN AMONG SUN-LIKE STARS WITH DIFFERENT LEVELS OF CHROMOSPHERIC AND CORONAL ACTIVITY

In Figure 1, the Sun and stars from different observed samples are presented on the Hertzsprung-Russell diagram. There are 1000 Sun-like stars from Wright et al. (2004) observed in the Program of Planet Search (open circles); 660 Sun-like stars from Arriagada (2011) observed in the Magellan Planet Search Program (asterisks) and 110 Sun-like stars and the Sun from Baliunas et al. (1995), observed in the Mount Wilson HK-project (filled circles). The solid line represents the Zero Age Main Sequence (ZAMS) on the Hertzsprung-Russell diagram.

Stars which are close to the ZAMS in Figure 1 have the lowest age among all stars shown: $\log(\text{Age}/\text{yr})$ is about 8–8.5. The older the star is, the farther it is from the ZAMS. Ages of all the stars in Figure 1 vary from 10^8 to 10^{10} yr.

We can also see that some stars significantly differ from the Sun in terms of their absolute magnitude M_V and color index $(B - V)$.

In different samples of stars from Planet Search Programs, some observers included a number of subgiants

with larger values of magnitude M_V among Sun-like stars on the main sequence. We try to exclude them from our analysis.

In Figure 2, one can see that stars have significantly different values of the S_{HK} -index, which determines their CA. There are stars from the Program of Planet Search (open circles), the Magellan Planet Search Program (asterisks) and 110 stars and the Sun from the HK-project (filled circles).

We cannot see a close relationship of CA in stars from our samples versus the color index in Figure 2.

Figures 1 and 2 show that Sun-like stars form a pattern, with a larger spread in their luminosities M_V and CA compared to the solar value.

It is important to note that the study of CA in stars is performed with very large data sets. Zhao et al. (2015) have studied a sample of $\sim 120\,000$ F, G and K stars from the LAMOST DR1 archive, which is an unprecedentedly large sample for the study the H&K CaII emission. The δS index was measured for these stars, calculated as the difference between standard S -index and a ‘zero’ emission line fitted using several of the least active stars across the whole range of T_{eff} . It was shown that active stars lie closer to the Galactic plane but inactive stars tend to be farther away from the Galactic plane.

For another large statistical sample – 2600 stars of the California Planet Search Program – the lower envelope of CA level S_{BL} (S_{HK} of the Basic Level) was defined as a function (polynomial fit) of $B - V$ for main sequence stars over the color range $0.4 < B - V < 1.6$, see Isaacson & Fischer (2010).

We show the S_{BL} dependence in Figure 2. It is seen that the Basic CA Level S_{BL} begins to rise when $B - V > 1$. Isaacson & Fischer (2010) believed that this increase in S_{BL} is due to the decrease of continuum flux for redder stars: S_{HK} is defined as the ratio of H&K CaII emission to the nearby continuum.

According to Isaacson & Fischer (2010), mean levels of CA (corresponding to the uniform Mount Wilson S -index) for stars of the spectral class F are higher than those of G-stars. On the other hand, for stars of K and M spectral classes, mean levels of CA are also higher than those of G-stars. However it can be noted that the level of CA in the Sun is slightly below the average level of CA in stars belonging to the main sequence.

The S_{HK} is affected by line blanketing in the continuum regions that increases with $(B - V)$ color index. This effect causes mistakes in the comparison of CaII activity for stars with different colors.

For describing the CA, it will be more correct to use the index $\log R'_{\text{HK}}$. The parameter $\log R'_{\text{HK}}$ is calculated from the mean S_{HK} and the $(B - V)$ color. It was originally formulated by Noyes et al. (1984). The sample of HK-project stars ranges from $\log R'_{\text{HK}} = -4.4$ (young stars) to -5.3 (old stars). The solar value of $\log R'_{\text{HK}} = -4.94$.

In our paper we use S_{HK} when we study the observed time series (“light curves” of the H&K CaII emission) but

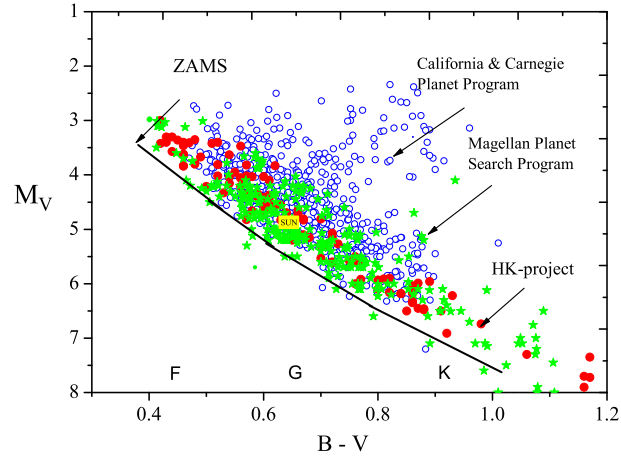


Fig. 1 The Sun among the Sun-like stars from different observational programs on the Hertzsprung-Russell diagram.

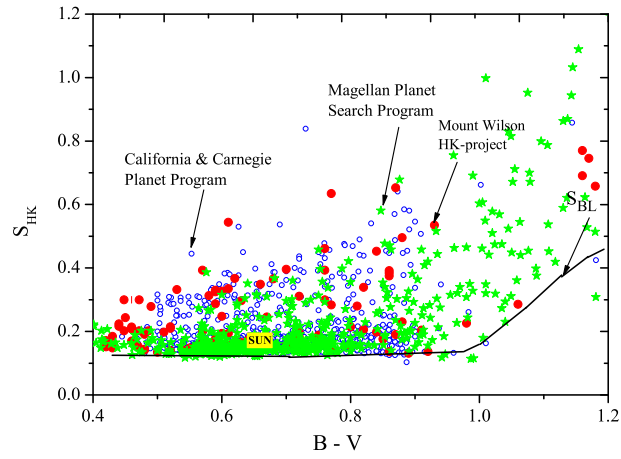


Fig. 2 CA of F, G, K and M stars from three observational programs.

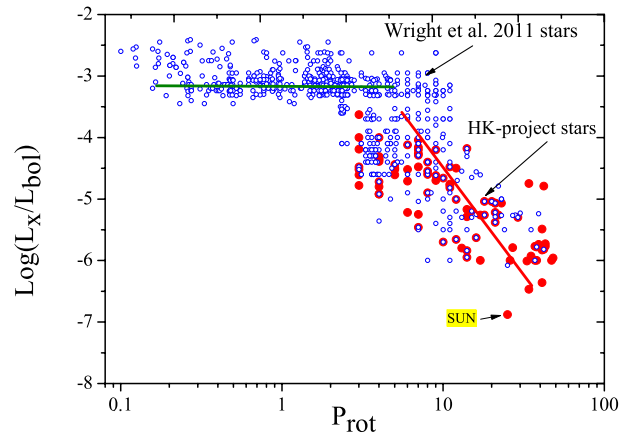


Fig. 3 X-ray to bolometric luminosity ratio plotted against rotation period.

below in this paper we will use $\log R'_{\text{HK}}$ as the more correct index of the CA.

In Sun-like stars of late spectral classes, X-rays are generated by the magnetically confined plasma known as the corona (see Vaiana et al. 1981), which is heated by the stellar magnetic dynamo. The observed decrease in the X-ray emission between pre-main sequence young stars and older stars can be attributed to the rotational spin-down of a star, driven by mass loss through a magnetized stellar wind (Skumanich 1972).

The magnetic fields of the Sun and solar-type stars are believed to be generated by flows of conductive matter. Such processes are commonly called a hydromagnetic dynamo or simply a dynamo.

The main parameter of solar and stellar dynamo models is the dynamo number $D = \alpha \Omega R^3 / \eta^2$, where Ω is the rotation rate of a star, R is its radius, η is the effective magnetic diffusivity, and the parameter α defines the intensity of field generation by the cyclonic convection (see Parker 1955; Vajnshtejn et al. 1980). The generation of magnetic fields is ultimately governed by hydrodynamic processes in stellar convection zones. The Sun's radiative interior is surrounded by a convection zone that occupies the outer 30% by radius; in most parts of this region the angular velocity Ω is constant on conical surfaces and there is a balance between Coriolis and baroclinic effects. At the base of the convection zone there is an abrupt transition in the tachocline to the almost uniformly rotating radiative zone. Superimposed on this pattern are zonal shear flows (torsional oscillations) that vary with the solar cycle, appearing as a branch of enhanced rotational velocity that coincides with the activity belt on the Sun and solar-type stars. As expected, the torsional oscillations on the Sun have an 11-year period, half of the underlying magnetic 22-year cycle. The main implications of the dynamo theory, as applied to stars, have revealed the main features of the cyclic behavior in the Sun and stars, but it involves ad hoc assumptions, which help us to compare the dynamo theory results with observations.

The nonlinear dynamo model allows us to explain the phenomenon of the irregular appearance of periods that show grand minima along with regular cycles of activity. In the nonlinear dynamo theory there is an important parameter – the critical dynamo number D_C for the field generation. The magnetic field decays for D below its critical value, namely when $D < D_C$ and rises with time for $D > D_C$. In a certain range of dynamo numbers, two types of solutions are possible: decaying oscillations of weak fields (known as Maunder minimum in solar observations) and magnetic cycles with a constant and large amplitude (known as the standard 11-year cycles), see Kitchatinov & Olemskoy (2010).

The rotation rate of the Sun and solar-type stars decreases with time (Skumanich 1972), with a feedback existing between the dynamo and rotation: the higher the magnetic activity is, the larger the rate of angular momentum loss. The reduction of the spin rate may ultimately

bring stars to the threshold of large-scale dynamo action. The states of low activity are actually only observed in old stars (Wright et al. 2004). If the proposed picture is valid, then observations can reveal a sharp decrease in reduction of the spin rates for old stars that exhibit grand minima in activity.

A relationship between the stellar rotation and X-ray luminosity L_X was first described by Pallavicini et al. (1981). In Figure 3 we show $\log(L_X/L_{\text{Bol}})$ versus P_{rot} for stars from the catalog of stars, the details of which are presented in Wright et al. (2011) – open circles, and for stars from the HK-project presented in Baliunas et al. (1995) – filled circles. In Wright et al. (2011), all X-ray luminosities of the stars from the catalog of 824 stars were converted to the ROSAT 0.1–2.4 keV energy band. The selected data of X-ray luminosities L_X/L_{Bol} of 80 HK-project stars were also taken from the ROSAT All-Sky Survey (Bruevich et al. 2001). This sample also includes the Sun using the values of $\log L_X/L_{\text{Bol}} = -6.88$ (for a medium level of activity) and $P_{\text{rot}} = 26.09$. Figure 3 demonstrates that there are two main regimes of coronal activity: a linear regime where activity increases with decreasing rotation period, and a saturated regime where the X-ray luminosity ratio is constant with $\log(L_X/L_{\text{Bol}}) = -3.13$ (see Wright et al. 2011, Wright et al. 2013).

We can see that the HK-project stars, which are not sufficiently young and active, belong to the linear regime in Figure 3. We can also note that the Sun confirms its place among Sun-like stars: it has a relatively low level of X-ray luminosity among all the stars in the studied sample.

Below in Figure 7b we also show the location of solar coronal activity among the coronal activity of stars in the HK-project. It can be noted that the Sun is at the place with the absolutely lowest level of coronal activity among Sun-like HK-project stars.

One can also note that solar photometric radiation changes very little in the activity cycle, less than 0.1%. The series of data from simultaneous monitoring of photometric and chromospheric H&K CaII emission from stars similar to the Sun in age and average activity level showed that there is an empirical correlation between the average stellar CA level and the photometric variability. In general, more active stars show larger photometric variability. The Sun is significantly less variable, which is indicated by an empirical relationship, see Shapiro et al. (2013). It was found that on a long timescale the position of the Sun on the diagram of photometric variability versus CA is not constant in time. So, Shapiro et al. (2013) suggested that the temporal mean solar variability might be in agreement with stellar data.

But at present, we can see that the Sun confirms its unique place among Sun-like stars: its photometric variability is unusually small. The observational verification has been confirmed in Lockwood et al. (2007): the Lowell observatory photometric observations of 33 stars from the HK-project revealed the fact that the photometric variability of the Sun during the cycle of magnetic activity is much

less than the photometric variability of other HK-project stars.

3 OBSERVATIONS OF HK-PROJECT STARS

It can be noted that among the databases of observations of Sun-like stars with known values of S_{HK} , the sample of stars from the HK-project was selected most carefully in order to study stars which are analogs of the Sun. Moreover, unlike different Planet Search Programs that observe Sun-like stars, the Mount Wilson Program was specifically developed for study of a Sun-like cyclical activity of main sequence F, G and K-stars (single) which are the closest to the “young Sun” and “old Sun.”

The duration of observations (more than 40 yr) in the HK-project has allowed detection and exploration of cyclical activity in these stars, similar to the 11-yr cyclical activity of the Sun. First O. Wilson began this program in 1965. He attached great importance to the long-standing systematic observations of cycles in the stars. Fluxes in passbands that were 0.1 nm wide and centered on the CaII H&K emission cores have been monitored in 111 stars of the spectral type F2-K5 on or near the main sequence in the Hertzsprung-Russell diagram (see Baliunas et al. 1995; Lockwood et al. 2007).

For the HK-project, stars were carefully chosen according to those physical parameters which are closest to the Sun: cold, single stars – dwarfs, belonging to the main sequence. Close binary systems were excluded.

Results of joint observations of the HK-project radiation fluxes and periods of rotation gave the opportunity for the first time in stellar astrophysics (Noyes et al. 1984) to detect the rotational modulation of the observed fluxes. This meant that on the surface of a star there are inhomogeneities which are dynamic and evolving in several periods of rotation of the stars around their axes. In addition, the evolution of the periods of rotation of the stars in time clearly pointed to the fact that the star’s differential rotations are similar to the Sun’s differential rotations.

The authors of the HK-project, by using frequency analysis of observations over 40 years, have discovered that the periods of 11-yr cyclic activity vary little in size for the same star (Baliunas et al. 1995; Lockwood et al. 2007). Durations of cycles vary from 7 to 20 yr for different stars. It was shown that stars with cycles represent about 30% of the total number of studied stars.

4 CYCLIC ACTIVITY OF HK-PROJECT STARS: FROM PERIODOGRAM TO WAVELET ANALYSIS

The evolution of active regions on a star on a timescale of about 10 yr is used to determine if the cyclic activity is similar to that in the Sun.

For 111 HK-project stars, periodograms were computed for each stellar record in order to search for activity cycles (Baliunas et al. 1995). The significance of the height of the tallest peak in the periodogram was estimated

by the false alarm probability (FAP) function (see Scargle 1982). The stars with cycles were classified as follows: if for the calculated $P_{\text{cyc}} \pm \Delta P$ the FAP function $\leq 10^{-9}$ then this star is in the “Excellent” class (P_{cyc} is the period of the cycle). If $10^{-9} \leq \text{FAP} \leq 10^{-5}$ then this star is in the “Good” class. If $10^{-5} \leq \text{FAP} \leq 10^{-2}$ then this star is in the “Fair” class. If $10^{-2} \leq \text{FAP} \leq 10^{-1}$ then this star is in the “Poor” class.

In Baliunas et al. (1995); Lockwood et al. (2007) the regular chromospheric cyclical activity of HK-project Sun-like stars was studied through the analysis of the power spectral density with Scargle’s periodogram method (Scargle 1982). It was pointed out that the detection of a periodic signal hidden by noise is frequently a goal in astronomical data analysis. So, Baliunas et al. (1995) determined if the periods of activity cycles in HK-project stars were similar to the 11-yr solar activity cycle. The significance of the height of the tallest peak in the periodogram was estimated by the FAP function. Among the 50 stars with detected cycles, only 13 stars (including the Sun) have been found which are characterized by the cyclic activity in the “Excellent” class.

We have illustrated the method of cyclic period calculation with Scargle’s periodogram technique on the example of the Sun. We obtained the periodogram of the yearly averaged relative sunspot number or Solar Sunspot Number (SSN) for observations conducted in 1800–2013.

In Figure 4 we present the relative sunspot number yearly averaged data set (top panel). It is known that direct observations of sunspots have been made only since 1850, and from 1700 to 1850 sunspot data have been taken from indirect estimates. This fact, as we will see below in Figure 5a, affects the quality of time-frequency analysis for data from 1700–1850.

In Figure 4 we show the Scargle’s periodogram of the relative sunspot number for the 1800–2013 data set (presented in the bottom panel). Our sample periodogram in Figure 4 shows that the main period of cycles is equal to approximately 11 yr. The level of the Power/Frequency or Power Spectral Density (PSD) as a function of frequency (1/year) for these observational data shows that the PSD value for the 11-year cycle is two times greater than for nearby PSD values. The fact that the peak of the 11-year periodicity is not very sharp shows that the period of the 11-year cycle is not constant: it changes (for two centuries of observations) from 10 to 12 yr.

In Figure 4 we marked the peaks corresponding to the smallest periods of the second order: a half-century cycle which was first discovered by Vitinskij et al. (1986), a 5.5-year cycle and a quasi-biennial cycle. The half-century cycle and 5.5-year peaks are not very pronounced (some percent) compared to the neighboring signals. The quasi-biennial peak (due to the fact that it is very weak in terms of power and is blurred due to the evolution of the period from 3.5 to 2 yr within a single 11-year cycle) is in general at the noise level. As one can see, the very obvious peak in the PSD, which corresponds to the 11-year cycle, has

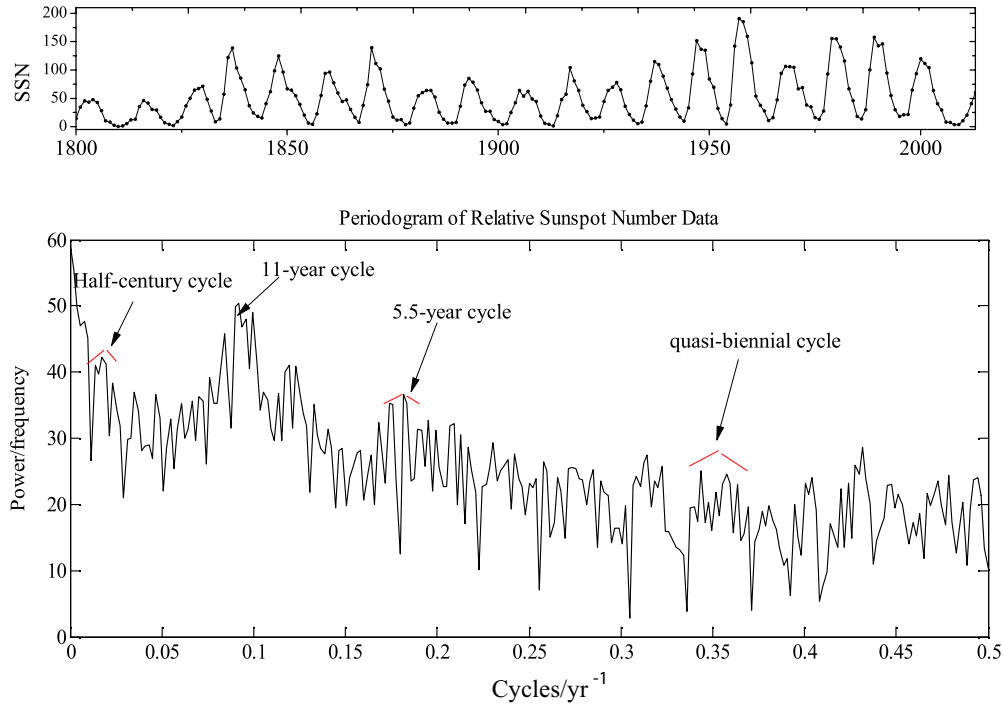


Fig. 4 The periodogram of the yearly averaged relative sunspot numbers for observations during 1800–2013.

a value only about two times greater than the surrounding background.

We can see that, unfortunately, this method only allows us to define a fixed set of main frequencies (which determine the presence of significant periodicities in the series of observations). In the case where values of periods change significantly during the interval of observations, the accuracy of determination of periods becomes worse. It is also impossible to obtain information about the evolution of the periodicity in time.

In Kolláth & Oláh (2009), different methods, such as short-term Fourier transform, wavelet and generalized time-frequency distributions, have been tested and used for analyzing temporal variations in timescales of long-term observational data which have information on the magnetic cycles of active stars and that of the Sun. Their time-frequency analysis of multi-decadal variability of the solar Schwabe (11-yr) and Gleissberg (century) cycles during the last 250 yr showed that one cycle (Schwabe) varies between limits, while the longer one (Gleissberg) continually increases. By analogy with the analysis of the longer solar record, the presence of a long-term trend may suggest an increase or decrease in a multi-decadal cycle that is presently unresolved in stellar records, which have short duration.

A wavelet technique has become popular as a tool for extracting local time-frequency information. The wavelet transform differs from traditional time-frequency analysis (Fourier analysis, Scargle's periodogram method) be-

cause of its efficient ability to detect and quantify multi-scale, non-stationary processes (Frick et al. 1997). The wavelet transform maps a one-dimensional time series $f(t)$ into a two-dimensional plane, which is related to time and frequency scales. Wavelets are the localized functions which are constructed based on one so-called mother wavelet $\psi(t)$. The choice of wavelet is dictated by signal or image characteristics and the nature of the application. Understanding properties of the wavelet analysis and synthesis, one can choose a mother wavelet function that is optimized for a particular application. Thus, we choose a complex Morlet wavelet which depends on two parameters: a bandwidth parameter and a wavelet center frequency. The Morlet wavelet allows one to get results with better spectral resolution. The Morlet mother wavelet function can be represented as $\psi(t) = e^{-t^2/a^2} e^{i2\pi t}$.

The standard algorithm of wavelet analysis as applied to astronomical observations of the Sun and stars was discussed in detail in Frick et al. (1997), Kolláth & Oláh (2009). The choice of the Morlet wavelet as the best mother wavelet $\psi(t)$ for astronomical data processing is discussed in Bruevich et al. (2014) on the basis of comparative analysis of results obtained using different mother wavelets.

The results of our solar data wavelet analysis are presented on the time-frequency plane (Fig. 5a,b,c). The notable crowding of horizontal lines on the time-frequency plane around the specific frequency indicates that the probability of stable cycles existing is higher for that frequency (cycle's duration) in accordance with the gradient bar to the right.

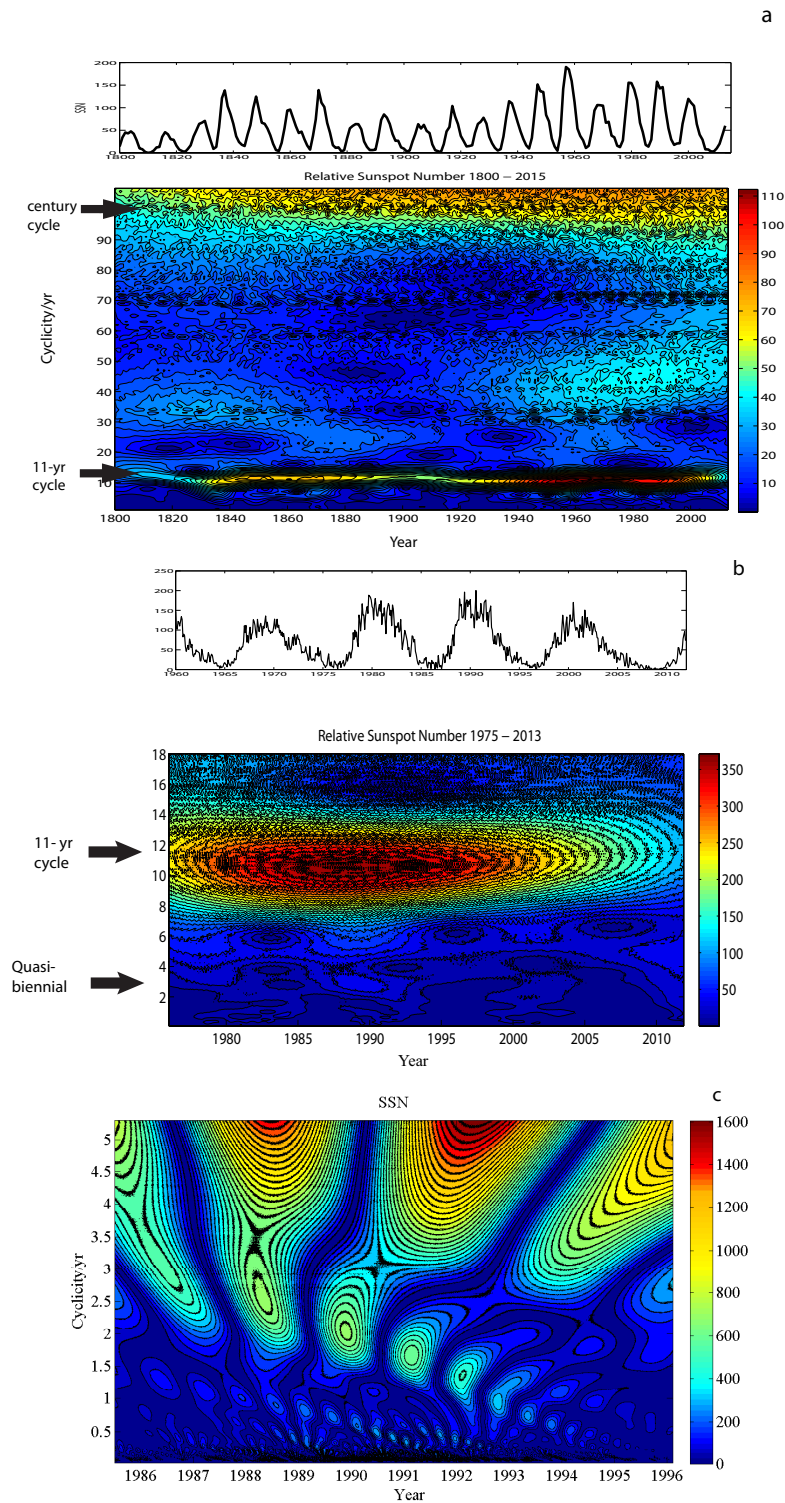


Fig. 5 Wavelet analysis of the relative sunspot numbers: (a) yearly averaged observations from 1700 to 2012; (b) monthly averaged observations from 1950 to 2012; (c) daily observations in the 22nd solar activity cycle.

In Figure 5 the results of the continuous wavelet transform analysis (with the help of a Morlet mother wavelet) applied to a time series of SSN are presented: Figure 5a corresponds to yearly averaged data, Figure 5b corresponds to monthly averaged data, and Figure 5c cor-

responds to daily data. The (X, Y) plane is the time-frequency plane of calculated wavelet-coefficients $C(a, b)$: parameter a corresponds to the Y -axis (Cyclicity, years), and parameter b corresponds to the X -axis (Time, years). The magnitudes of $C(a, b)$ coefficients, characterizing the

probability amplitude of a regular cyclic component localized at the point (a, b), are represented by the Z axis.

In Figure 5 we see the projection of $C(a, b)$ to (a, b) or the (X, Y) plane. This projection on the plane (a, b) with isolines allows us to trace changes in the coefficients on various scales in time and reveal a picture of local extrema associated with these surfaces. It is the so-called skeleton of the structure of the analyzed process. We can also note that the configuration of the Morlet wavelet is very compact in frequency, which allows us to determine the localization of instantaneous frequency of observed signal most accurately (compared to other mother wavelets).

Figure 5a presents the results of wavelet analysis of the same yearly averaged sunspot number data set as in Figure 4. The cycles with century, half-century and 11-yr durations are marked with arrows. In Figure 5b we show the results of wavelet analysis of the monthly averaged sunspot number data set. The cycles with 11-yr and quasi-biennial durations are marked in this plot. Note that for the study of cycles on a shorter timescale (Fig. 5b) we use more detailed observations of the Sun.

Figure 5a confirms the known fact that the period of the main solar activity cycle is about 11-yr in the 19th century and is about 10 yr in the 20th century. It is also known that the abnormally long 23rd cycle of solar activity ended in 2009 and lasted about 12.5 yr. We can see all these facts in Figures 5a and b. Thus, it can be argued that the value for a period of the main cycle of solar activity during the past 200 yr is not constant and varies by 15%–20%.

In Figure 5c we show the results of wavelet analysis of daily SSN data in solar cycle 22. We analyzed those data on a timescale which is equal to several years and identified the second order periodicity such as 5.5 yr and quasi-biennial as well as their temporal evolution.

In Oláh et al. (2009) a study of time variations in cycles of 20 active stars based on decades of observations (long photometric or spectroscopic) with a method of time-frequency analysis was done. They found that cycles of Sun-like stars show systematic changes. The same phenomenon can be observed for the cycles of the Sun.

Oláh et al. (2009) found that fifteen stars definitely show multiple cycles, but the records of the rest are too short to verify a timescale for a second cycle. For six HK-project stars (HD 131156A, HD 131156B, HD 100180, HD 201092, HD 201091 and HD 95735), multiple cycles were detected. Using wavelet analysis, the following results (other than periodograms from Baliunas et al. 1995) were obtained:

HD 131156A shows variability on two timescales: the shorter cycle is about 5.5-yr, and a longer-period of variability is about 11 yr.

For HD 131156B only one long-term periodicity has been determined.

For HD 100180 a variable cycle of 13.7-yr appears in the beginning of the record; the period decreases to 8.6-yr by the end of the record. The results in the beginning of the dataset are similar to those published by Baliunas et al.

(1995), who found two cycles, which are equal to 3.56 and 12.9-yr.

The record for HD 201092 also exhibits two activity cycles: one is equal to 4.7-yr, and the other has a timescale of 10–13 yr.

The main cycle, seen in the record of HD 201091, has a mean length of 6.7-yr, which slowly changes between 6.2 and 7.2-yr. A shorter, significant cycle is found in the first half of the record with a characteristic timescale of 3.6-yr.

The stronger cycle of HD 95735 is 3.9-yr. A longer, 11-yr cycle is also present with a smaller amplitude.

In our paper we have applied wavelet analysis for partially available data from the records of relative CaII emission fluxes - the variation of S_{HK} for observation sets from 1965–1992 by Baliunas et al. (1995) and observations from 1985–2002 by Lockwood et al. (2007). We used the detailed plots of S_{HK} time dependencies: each point of the record of observations, which we processed in this paper using the wavelet analysis technique, corresponds to averaged values over three months for S_{HK} .

In this paper we have studied five HK-project stars with cyclic activity from the “Excellent” class: HD 10476, HD 81809, HD 103095, HD 152391 and HD 160346, and the star HD 185144 with no cyclicity.

We used the complex Morlet wavelet $1.5 - 1$ which can most accurately determine the dominant cyclicity as well as its evolution in time in solar data sets at different wavelengths and spectral intervals (Bruevich & Yakunina 2015).

We hope that wavelet analysis can help to study the temporal evolution of CA cycles in these stars. Three-month averaging also helps us to avoid the modulation of observational S_{HK} data from stars’ rotations.

In Figure 6 we present our results for cycles of six HK-project stars:

HD 81809 has a mean cycle duration of 8.2-yr, which slowly changes between 8.3-yr in the first half of the record and 8.1-yr in the middle and the end of the record while Baliunas et al. (1995) found 8.17-yr.

HD 103095 has a mean cycle duration of 7.2-yr, which slowly changes between 7.3-yr in the first half of the record, 7.0-yr in the middle and 7.2-yr in the end of the record while Baliunas et al. (1995) found 7.3-yr.

HD 152391 has a mean cycle duration of 10.8-yr, which slowly changes between 11.0-yr in the first half of the record and 10.0-yr in the end of the record while Baliunas et al. (1995) found 10.9-yr.

HD 160346 has a mean cycle duration of 7.0-yr which does not change during the record in agreement with 7.0-yr estimated by Baliunas et al. (1995).

HD 10476 has a mean cycle duration of 10.0-yr in the first half of the record, then it sharply changes to 14-yr, but Baliunas et al. (1995) found 9.6-yr. After changing the high amplitude cycle’s period from 10-yr to 14-yr in 1987, the low amplitude cycle still had a 10.0-yr period - we can see two activity cycles. Baliunas et al. (1995) estimated the HD 10476 cycle to be 9.6-yr.

HD 185144 has a mean cycle duration of 7-yr which changes between 8-yr in the first half of the record and 6-yr in the end of the record while Baliunas et al. (1995) have not found a well-pronounced cycle.

In Oláh et al. (2009), multiple cycles were found for the stars HD 13115A, HD 131156B and HD 93735, for which no cycles were found in Baliunas et al. (1995). For the stars in the “Excellent” class HD 201091 and HD 201092, cycle periods found in Baliunas et al. (1995) were confirmed and the shorter cycles (similar to solar quasi-biennial) were also determined.

Oláh et al. (2009) have concluded that all the stars from their pattern of cool main sequence stars have cycles and most of the cycle durations change systematically.

However we can see that the stars in the “Excellent” class have relatively constant cycle durations – for these stars the periods of their cycles calculated in Baliunas et al. (1995) and those found with the use of the wavelet analysis are the same.

A similar picture can be seen for the Sun: the long-term behavior of the sunspot group numbers has been analyzed using a wavelet technique by Frick et al. (1997) who plotted changes in the Schwabe cycle (length and strength) and studied the grand minima. The temporal evolution of the Gleissberg cycle can also be seen in the time-frequency distribution of the solar data. According to Frick et al. (1997), the Gleissberg cycle is as variable as the Schwabe cycle. It has two higher amplitude occurrences: the first one is around 1800 (during the Dalton minimum), and the next one is around 1950. They found a very interesting fact – the continuous decrease in frequency (increase of period) of the Gleissberg cycle. Although near 1750 the cycle duration was about 50 yr, it lengthened to approximately 130 yr by 1950.

In the late part of the 20th century, some solar physicists began to examine the variations of relative sunspot numbers with different methods, not only in the high amplitude 11-yr Schwabe cycle but also in low amplitude cycles approximately equal to a half (5.5-yr) and a quarter (quasi-biennial) of the period of the main 11-yr cycle, see Vitinskij et al. (1986). The periods of the quasi-biennial cycles vary considerably within one 11-yr cycle, decreasing from 3.5 to 2 yr (see Fig. 5b,c), which complicates the study of such periodicity with the periodogram method.

Using methods of frequency analysis of signals, quasi-biennial cycles have been studied not only for the relative sunspot number, but also for 10.7 cm solar radio emission and for some other indices of solar activity, see Bruevich & Yakunina (2015). It was also shown that the cyclicity on the quasi-biennial timescale often takes place among stars with 11-yr cyclicity, see Bruevich & Kononovich (2011).

Cyclicity similar to the solar quasi-biennial was also detected for Sun-like stars from direct observations. In Morgenthaler et al. (2011), results of direct observations of magnetic cycles in 19 Sun-like stars of F, G, K spectral classes within 4 yr were presented. Stars in this sample are characterized by masses between 0.6 and 1.4 solar

masses and by rotation periods between 3.4 and 43 days. Observations were made using the NARVAL spectropolarimeter (Pic du Midi, France) between 2007 and 2011. It was shown that for the stars τ Boo and HD 78366 in this sample (the same ones from the Mount Wilson HK-project), the cycle lengths derived by CA from Baliunas et al. (1995) seem to be longer than those derived by spectropolarimetry observations from Morgenthaler et al. (2011). They suggest that this apparent discrepancy may be due to the different temporal sampling inherent to these two approaches, so that the sampling adopted at Mount Wilson may not be sufficiently tight to unveil short activity cycles. They hope that future observations of the Pic du Midi stellar sample will allow them to investigate longer timescales of stellar magnetic evolution.

For Sun-like F, G and K stars observed with *Kepler*, “shorter” chromosphere cycles with periods of about two years have also been found (see Metcalfe et al. 2010; García et al. 2010).

We assume that precisely these quasi-biennial cycles were identified in Morgenthaler et al. (2011): τ Boo and HD 78366 are also part of the HK-project. These stars have cycles similar to the quasi-biennial solar cycles with periods of a quarter of the duration of the periods defined in Baliunas et al. (1995).

Note that in case of the Sun, the amplitude of variations of the radiation in quasi-biennial cycles is substantially less than the amplitude of variations in the main 11-yr cycles. We believe that this fact is also true for all Sun-like stars in the HK-project and in the same way for τ Boo and HD 78366.

The quasi-biennial cycles cannot be detected with Scargle’s periodogram method. But methods of spectropolarimetry from Morgenthaler et al. (2011) allowed detecting the cycles with 2 and 3-yr periods. Thus, spectropolarimetry is a more accurate method for detection of cycles with different periods and with low amplitudes of variations.

So, the need for wavelet analysis of HK-project observational data is also dictated by the fact that the application of the wavelet method to these observations will help: (1) to find cyclicities with periods equal to a half and a quarter of the main high amplitude cyclicity; (2) to clarify periods of high amplitude cycles and to follow their evolution in time; (3) to find other stars with cycles for which cycles were not determined using the periodogram method due to strong variations of the period as in the case of HD 185144.

The analysis of cyclic activity in Sun-like stars using Scargle’s periodogram method in Baliunas et al. (1995) and wavelet analysis simultaneously showed that the ranking of stars into classes according to the quality of their cycles (“Excellent”, “Good”, “Fair” and “Poor”) is very important in the study of stellar cycles.

Wavelet analysis helped us to understand why stars in “Fair” and “Poor” classes differ from stars in “Excellent” and “Good” classes: the main peak in their periodograms

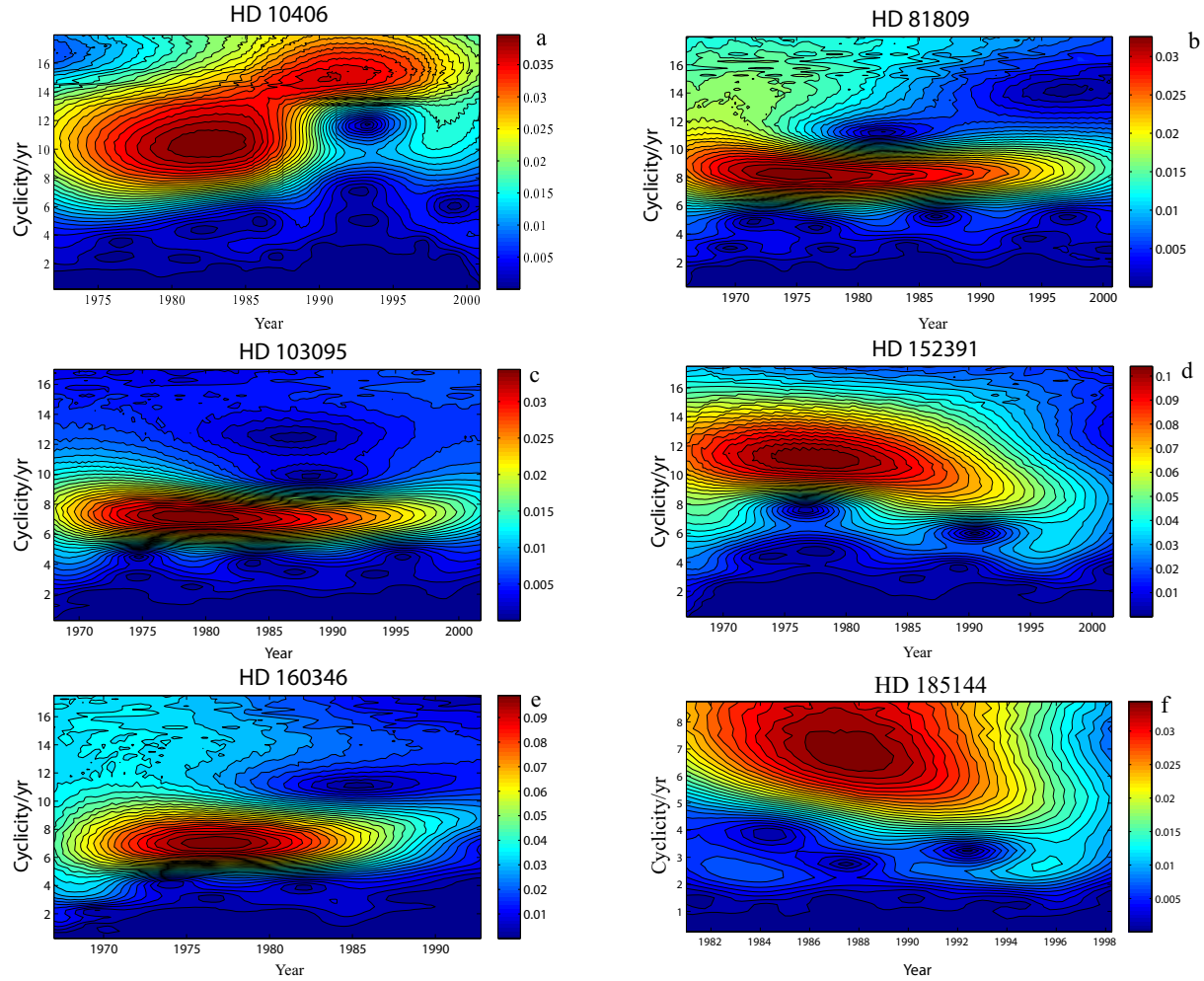


Fig. 6 Wavelet analysis of HK-project stars using the complex Morlet wavelet 1.5–1. Observations from 1969 to 2002: (a) HD 10476, (b) HD 81809, (c) HD 103095, (d) HD 152391, (e) HD 160346, and (f) HD 185144.

is greatly expanded due to strong variations of the cycle’s duration.

As it turned out, the differentiation of stars in terms of cycles into “Excellent,” “Good,” “Fair” and “Poor” classes is very important: stars with stable cycles (“Excellent” and “Good”) and stars with unstable cycles (“Fair” and “Poor”) are related to different groups in the graphs of $\log R'_{\text{HK}}$ versus $(B - V)$, $\log L_X/L_{\text{Bol}}$ versus $(B - V)$, and P_{cyc} versus Age, see Figure 7 and Figure 8 below.

5 CHROMOSPHERIC AND CORONAL ACTIVITY OF HK-PROJECT STARS WITH DIFFERENT SPECTRAL CLASSES WITH CYCLES

Processes, that determine complex phenomena of stellar activity and cover practically the whole atmosphere from the photosphere to the corona, occur differently among Sun-like stars belonging to different spectral classes.

The Mount Wilson HK-project observational data allow us to study the Sun-like cyclic activity of stars simulta-

neously with their chromospheric and coronal activity. The selected data of X-ray luminosities $\log L_X/L_{\text{Bol}}$ of 80 HK-project stars were taken from the ROSAT All-Sky Survey, see Bruevich et al. (2001).

As noted earlier by Baliunas et al. (1995); Lockwood et al. (2007), the average CA of the stars, or rather the values of S_{HK} and also of $\log R'_{\text{HK}}$, varies (increases) with the increase of the color index $(B - V)$, see Figure 2 and Figure 7a.

Our polynomial regression analysis of HK-project stars showed that there is a relation which is described by the following formula

$$\log R'_{\text{HK}} = -5.03 + 0.637 \times (B - V) - 0.358 \times (B - V)^2. \quad (1)$$

Let us denote the right part of Equation (1) as $F(B - V)$.

We consider the stars which have $\log R'_{\text{HK}} > F(B - V)$ to be characterized by a high level of CA, and stars with $\log R'_{\text{HK}} \leq F(B - V)$, by a low level of CA, see Figure 7a.

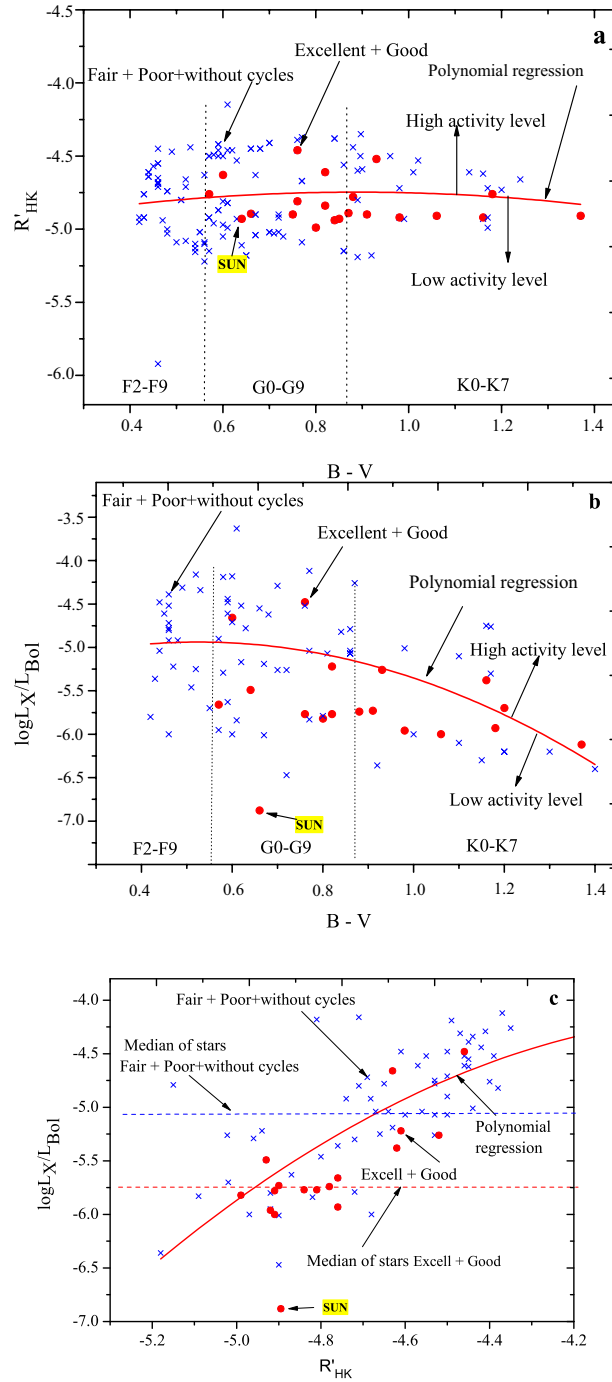


Fig. 7 HK-project stars with observations from 1969 to 1994. (a) $\log R'_{HK}$ versus $(B - V)$, (b) $\log L_X/L_{Bol}$ versus $(B - V)$, (c) $\log L_X/L_{Bol}$ versus $\log R'_{HK}$. Solid line – polynomial regression, “Excellent” + “Good” stars– filled circles, “Fair” + “Poor” stars and stars without cycles– crosses. Dashed lines – median values for stars of “Fair” + “Poor” + “Var” classes (upper dashed line) and “Excellent” + “Good” classes (lower dashed line).

Next, we have analyzed all 110 stars from the HK-project and the Sun to determine which kind of level of CA corresponds to one or another star. We will consider these results further in the comparative analysis of stars in different spectral classes, see Table 1.

For 80 stars, the coronal radiation of which we know from the ROSAT data, we also apply polynomial regression analysis and obtain the following relationship between the X-ray luminosity, normalized to the bolometric lumi-

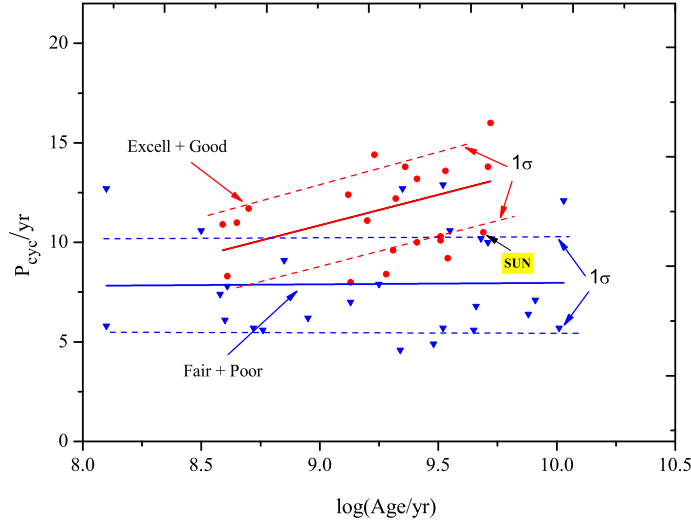


Fig. 8 P_{cyc} versus stellar age for stars in the HK-project. The regressions for the full sample (*lower dashed line*) and for stars with cycles of the “Excellent” + “Good” classes (*upper solid line*) are shown. For both regressions the dotted lines indicate the intervals corresponding to a 1σ standard deviation.

nosity, and the color index ($B - V$)

$$\log L_X/L_{\text{Bol}} = -5.45 + 1.95 \times (B - V) - 1.85 \times (B - V)^2. \quad (2)$$

Let us denote the right hand side of Equation (2) as $P(B - V)$. By analogy with the analysis of CA in stars, we consider the stars with $\log L_X/L_{\text{Bol}} > P(B - V)$ to be characterized by a high level of coronal activity, and stars with $\log L_X/L_{\text{Bol}} \leq P(B - V)$, by a low level of coronal activity, see Figure 7b.

As noted above, in the case of CA, a direct correlation takes place: with the increase of the color index ($B - V$) the average value of CA as measured by S_{HK} increases, see Isaacson & Fischer (2010). When we use $\log R'_{\text{HK}}$ as the index of the CA we see the other trend - with the increase of the color index ($B - V$) the average value of $\log R'_{\text{HK}}$ is almost constant, see Figure 7a. When we consider the dependence of X-ray radiation of stars from ($B - V$), an inverse correlation takes place: with the increase of the color index ($B - V$), the average value of $\log L_X/L_{\text{Bol}}$ decreases, see Figure 7b.

Figure 7a and 7b also demonstrates that stars with cycles of “Excellent” and “Good” classes are mostly characterized by the low level of chromospheric and coronal activity (about 70%), as opposed to stars with cycles of “Fair” and “Poor” classes which are mostly characterized by the high level of chromospheric and coronal activity (about 75%).

Note that most stars, characterized by increased CA, also have increased coronal activity. About 15% of stars, including the Sun, are characterized by coronal activity that is significantly lower than the value which should correspond to its CA, see Figure 7c. The regression line in

Figure 7c divides the stars with relatively high and relatively low $\log L_X/L_{\text{Bol}}$. It is seen that stars with no cycles (“Var”) and stars with poorly pronounced cyclical activity (“Fair” + “Poor”) are characterized by relatively high fluxes of coronal radiation (median value corresponds to the value of $\log L_X/L_{\text{Bol}} = -5.05$). The stars, belonging to classes “Excellent” + “Good,” are on average characterized by lower level fluxes of coronal radiation (a median value corresponds to the value of $\log L_X/L_{\text{Bol}} = -5.75$).

The existence or absence of a pronounced cyclicity, as well as the quality of the identified cycles (belonging to classes “Excellent,” “Good,” “Fair” and “Poor”), for F, G and K stars varies significantly, see Table 1.

Bruevich et al. (2001) noted the difference between stars in “Excellent,” “Good,” “Fair” and “Poor” classes from a perspective of presence and degree of development of underlying photospheric convective zones in stars with different color index ($B - V$).

In Table 1 we can see that for our sample of HK-project stars the coronal activity is higher in stars of the spectral class F, due to their total increased atmospheric activity (as compared to stars of spectral classes G and K). This conclusion is consistent with the findings of Kunte et al. 1988 in which it was found that $\log L_X/L_{\text{Bol}}$ is well correlated (decreases) with the age of stars. But on the other hand, G and K HK-project stars in our study are older than F stars, which is evident from their slower rotation.

Thus, we can note here (as shown in Table 1) that the quality of CA cycles (the ratio of the total number of stars belonging to classes with a well-defined cyclicity “Excellent” + “Good” to the number of stars with less than a certain cyclicity “Fair” + “Poor”) essentially differs for stars of different spectral classes F, G and K.

Table 1 Comparative Analysis of Cycles of Stars and the Quality of Their Cyclicities for Stars of Different Spectral Classes

| Interval of spectral classes | F2–F9 | G0–G9 | K0–K7 |
|---|-----------|-----------|-----------|
| $\Delta(B - V)$ | 0.42–0.56 | 0.57–0.87 | 0.88–1.37 |
| Total number of stars in spectral interval | 39 | 44 | 27 |
| Number of stars with known values of L_X/L_{Bol} | 26 | 32 | 22 |
| Relative number of stars with increased coronal activity | 61% | 42% | 36% |
| Relative number of stars with increased CA | 56% | 46% | 48% |
| Relative number of stars with CA cycles | 25% | 40% | 72% |
| Quality of chromospheric cycles “Excell+Good”/“Fair+Poor” | 0/10 | 7/10 | 14/4 |

Different tests of the dependency of the cycle period (with durations on various timescales from seconds in the asteroseismic analysis to several years in studies of dynamo processes) on different parameters of Sun-like stars have been performed, see Morgenthaler et al. (2011); García et al. (2010); García et al. (2014); Mathur et al. (2012); Metcalfe et al. (2010).

We have analyzed the dependence of the duration of a star’s magnetic cycle duration on its age. Cycle durations were taken from Baliunas et al. (1995). Unfortunately, we have a very limited stellar sample (Lockwood et al. 2007). Stellar ages were calculated according to Wright et al. (2004) as a function of the CA.

In Figure 8, the connection of P_{cyc} with ages of stars is shown. The scatter of points around the regression line is very large. For stars with cycles in the “Excellent” + “Good” classes with the increase of age (or various parameters connected with age) the duration of cycles increases by about 20% with an increase of $\log(\text{Age}/\text{yr})$ from 8.5 to 10. The stars with cycles in the “Fair” + “Poor” classes show no dependence of P_{cyc} on age.

For carrying out a high quality examination of cycles for Sun-like stars, the problem of determination of P_{cyc} as accurately as possible, using frequency-time (wavelet) analysis, becomes possible.

6 CONCLUSIONS

- The quality of cyclic activity, similar to the solar 11-yr one, is significantly improved (from “Fair + Poor” to “Excellent + Good”) in G and K-stars as compared to F-stars. The 11-yr cyclicity of F-stars (detected only in every fourth case) is determined with a lower degree of reliability.
- We show that for the interpretation of observations the use of modern methods of wavelet analysis is required. The nature of the cyclic activity of Sun-like stars is very similar to the Sun’s one: along with main cycles there are quasi-biennial cycles. Periods of solar quasi-biennial cycles evolve during one main 11-yr cy-

cle from 2 to 3.5 yr which complicates their detection with the periodogram technique. Our conclusion about quasi-biennial cycles for stars is supported by the direct observation of cycles with the duration of 2–3 yr for τ Boo and HD 78366 by Morgenthaler et al. (2011) and earlier detection of cycles with durations of 11.6 and 12.3 yr by Baliunas et al. (1995) for the same stars.

- The level of CA of the Sun is consistent with that of HK-project stars, which have well-defined cycles of activity (“Excellent + Good”) and similar color indexes.
- The stars belonging to “Excellent” + “Good” classes are on average characterized by lower level fluxes of coronal radiation (the median value corresponds to the value of $\log L_X/L_{\text{Bol}} = -5.05$), while stars without cycles have higher level fluxes of coronal radiation (the median value corresponds to the value of $\log L_X/L_{\text{Bol}} = -5.75$).
- There is great interest now in the problem of finding planets in the habitable zone which is the region around a star where a planet with sufficient atmospheric pressure can maintain liquid water on its surface. We believe that in the search for life on exoplanets, close attention should be paid to the characteristics of our Sun: a low level of variability in the photospheric radiation simultaneously with a very low level of the coronal radiation. So, the search for extraterrestrial life should be conducted simultaneously with the search for “planets in the habitable zone” and “stars that are comfortable for life,” such as the Sun.

References

- Arriagada, P. 2011, *ApJ*, 734, 70
- Baliunas, S. L., Donahue, R. A., Soon, W. H., et al. 1995, *ApJ*, 438, 269
- Bruevich, E. A., Katsova, M. M., & Sokolov, D. D. 2001, *Astronomy Reports*, 45, 718
- Bruevich, E. A., & Kononovich, E. V. 2011, *Moscow University Physics Bulletin*, 66, 72
- Bruevich, E. A., Bruevich, V. V., & Yakunina, G. V. 2014, *Sun and Geosphere*, 8, 91
- Bruevich, E. A., & Yakunina, G. V. 2015, *Moscow University Physics Bulletin*, 70, 282
- Frick, P., Baliunas, S. L., Galyagin, D., Sokoloff, D., & Soon, W. 1997, *ApJ*, 483, 426
- García, R. A., Mathur, S., Salabert, D., et al. 2010, *Science*, 329, 1032
- García, R. A., Ceillier, T., Salabert, D., et al. 2014, *A&A*, 572, A34
- Isaacson, H., & Fischer, D. 2010, *ApJ*, 725, 875
- Kitchatinov, L. L., & Olemskoy, S. V. 2010, *Astronomy Letters*, 36, 292
- Kolláth, Z., & Oláh, K. 2009, *A&A*, 501, 695
- Kunte, P. K., Rao, A. R., & Vahia, M. N. 1988, *Ap&SS*, 143, 207

- Lockwood, G. W., Skiff, B. A., Henry, G. W., et al. 2007, *ApJS*, 171, 260
- Mathur, S., Metcalfe, T. S., Woitaszek, M., et al. 2012, *ApJ*, 749, 152
- Metcalfe, T. S., Monteiro, M. J. P. F. G., Thompson, M. J., et al. 2010, *ApJ*, 723, 1583
- Morgenthaler, A., Petit, P., Morin, J., et al. 2011, *Astronomische Nachrichten*, 332, 866
- Noyes, R. W., Hartmann, L. W., Baliunas, S. L., Duncan, D. K., & Vaughan, A. H. 1984, *ApJ*, 279, 763
- Oláh, K., Kolláth, Z., Granzer, T., et al. 2009, *A&A*, 501, 703
- Pallavicini, R., Golub, L., Rosner, R., et al. 1981, *ApJ*, 248, 279
- Parker, E. N. 1955, *ApJ*, 122, 293
- Scargle, J. D. 1982, *ApJ*, 263, 835
- Shapiro, A. I., Schmutz, W., Cessateur, G., & Rozanov, E. 2013, *A&A*, 552, A114
- Skumanich, A. 1972, *ApJ*, 171, 565
- Vaiana, G. S., Cassinelli, J. P., Fabbiano, G., et al. 1981, *ApJ*, 245, 163
- Vajnshtejn, S. I., Zel'dovich, Y. B., & Ruzmajkin, A. A. 1980, *Turbulent Dynamo in Astrophysics*. (Moskva: Nauka, in Russian)
- Vaughan, A. H., & Preston, G. W. 1980, *PASP*, 92, 385
- Vitinskij, Y. I., Kopetskij, M., & Kuklin, G. V. 1986, *Statistics of the Spot-forming Activity of the Sun*. (Moskva: Nauka, in Russian)
- Wright, J. T., Marcy, G. W., Butler, R. P., & Vogt, S. S. 2004, *ApJS*, 152, 261
- Wright, N. J., Drake, J. J., Mamajek, E. E., & Henry, G. W. 2011, *ApJ*, 743, 48
- Wright, N. J., Drake, J. J., Mamajek, E. E., & Henry, G. W. 2013, *Astronomische Nachrichten*, 334, 151
- Zhao, J.-K., Oswalt, T. D., Chen, Y.-Q., et al. 2015, *RAA (Research in Astronomy and Astrophysics)*, 15, 1282